Supplementary Information for Publication

Negative Thermal Expansion in Cubic $FeFe(CN)_6$ Prussian Blue Analogues

Naike Shi [a, b], Qilong Gao [a, b], Andrea Sanson [c], Qiang Li [a, b], Longlong Fan [d], Yang Ren [e], Luca Olivi [f], Jun Chen *[a, b] and Xianran Xing [a, b]

[a]*Beijing Advanced Innovation Center for Materials Genome Engineering, University of Science and Technology Beijing, Beijing 100083, China*

[b]*Department of Physical Chemistry, University of Science and Technology Beijing, Beijing 100083, China*

[c]*Department of Physics and Astronomy, University of Padova, Padova I-35131, Italy*

[d]*College of Physics and Materials Science, Tianjin Normal University, Tianjin 300387, China*

[e]*Argonne National Laboratory, X-ray Science Division, Argonne, Illinois 60439, United States*

[f]*Elettra Sincrotrone Trieste, 34149 Basovizza, Italy*

Correspondence and requests for materials should be addressed to Jun Chen (email: junchen@ustb.edu.cn).

Supporting Figures and Tables

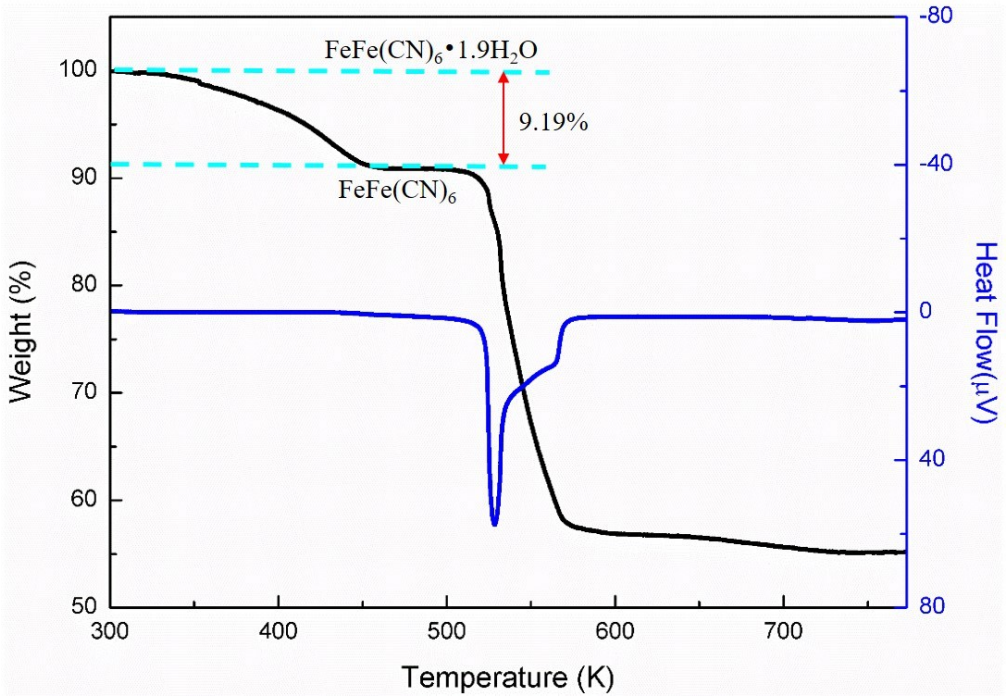

Figure S1. TG-DSC curves of $FeFe(CN)_6 \cdot 1.9H_2O$ measured at a rate of 1 K/min in an inert Ar atmosphere.

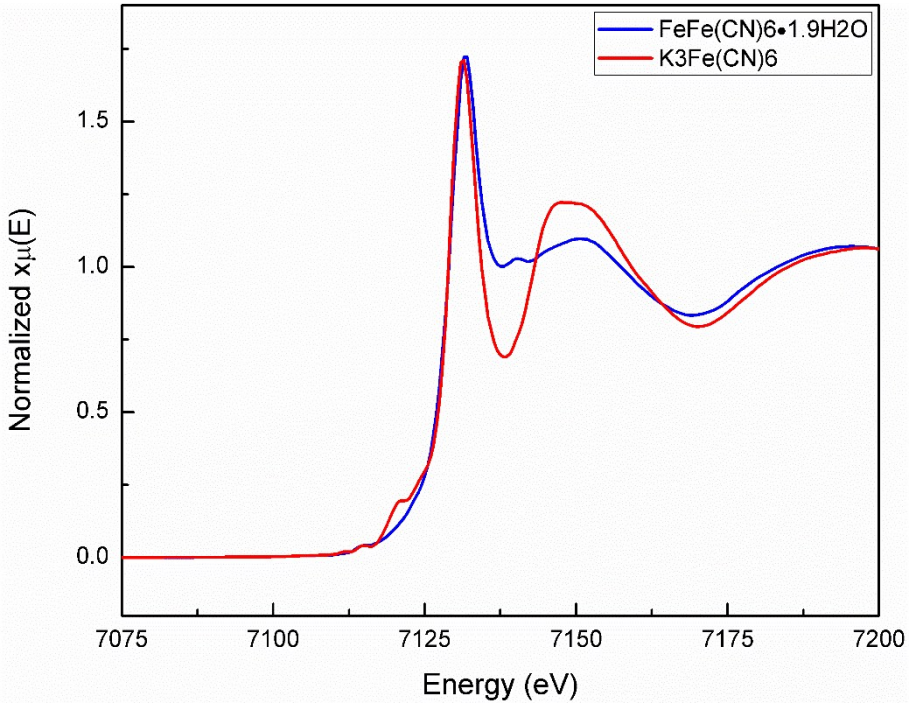

Figure S2. Comparison of Fe K-edge XANES spectra of $FeFe(CN)_6 \cdot 1.9H_2O$ and standard sample $K_3Fe(CN)_6$ at room temperature, indicating the state of Fe in $FeFe(CN)_6$ is same as that in $K_3Fe(CN)_6$, corresponding to Fe^{3+}.

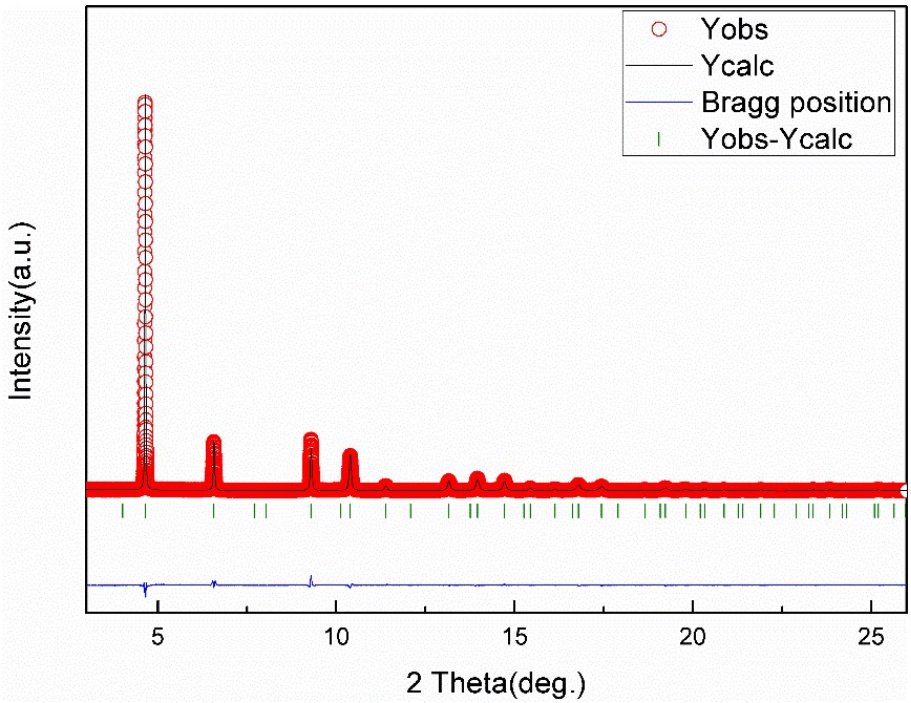

Figure S3. Structure refinements of the high-resolution SXRD data of $FeFe(CN)_6$ collected at room temperature. $R_p = 7.36$, $R_{wp} = 9.78$, $R_{exp} = 6.57$, $\chi^2 = 2.22$.

Table S1. Negative thermal expansion properties of isotropic NTE materials

Materials	**α/ 10^{-6} K^{-1}**	**T/K**	**Ref.**
ScF_3	-3.1	300-800	1
$FeZrF_6$	-3.24	298-675	2
$CaZrF_6$	-6.69	298-675	2
$ZrMo_2O_8$	-5	0-600	3
ZrV_2O_7	-6.7	473-873	4
ZrW_2O_8	-8.7	20-430	5
$NiPt(CN)_6$	-1.02	100-330	6
$FeCo(CN)_6$	-1.47	4.2-300	7
$Rb_{0.78}Fe[Fe(CN)_6]_{0.832}•8H_2O$	-2.1	100-300	8
$GaFe(CN)_6$	-3.95	100-475	9
$FePt(CN)_6$	-4	100-315	6
$CdPt(CN)_6$	-10.02	100-240	6
$Zn(CN)_2$	-16.9	25-375	10
$Cd(CN)_2$	-20.4	150-375	10
$FeFe(CN)_6$	-4.26	100-450	This work

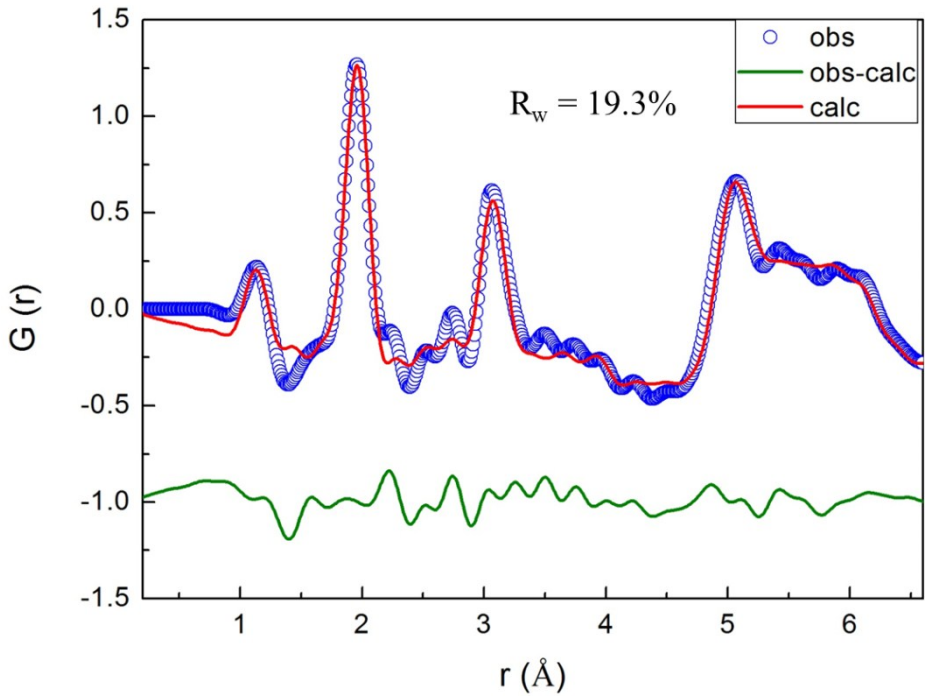

Figure S4. PDF fit of synchrotron radiation X-ray total scattering obtained at 475 K for the $FeFe(CN)_6$ at low r values (0.2-6.6 Å).

EXAFS data analysis details

The EXAFS signals, extracted according to well-established procedures, [11] are shown in Fig. S5. In order to separate the contributions of the different coordination shells, the k-weighted EXAFS signals were Fourier transformed (FT) in the k range 2-12 $Å^{-1}$ using a Gaussian window (Fig. S6). The EXAFS scattering paths contributing to the FT structure between about 0.75 and 3.25 Å in the FT, calculated using the FEFF code, [12] are listed in Table S2. A non-linear best fit to the experimental spectra was then performed in the r-space between 0.75 and 3.25 Å (bold-dashed lines in Fig. S6) by using the FEFFIT package. [13] Finally, the absolute values of the parallel and perpendicular MSRDs have been obtained through the correlated Einstein model. [14]

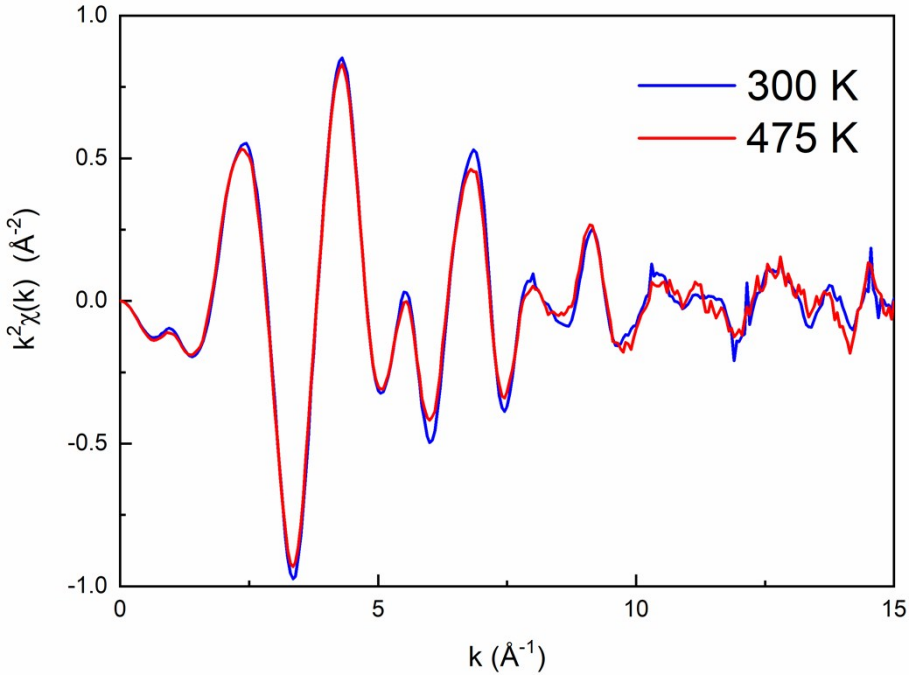

Figure S5. Fe K-edge EXAFS signals of $FeFe(CN)_6$ at room temperature and 475 K.

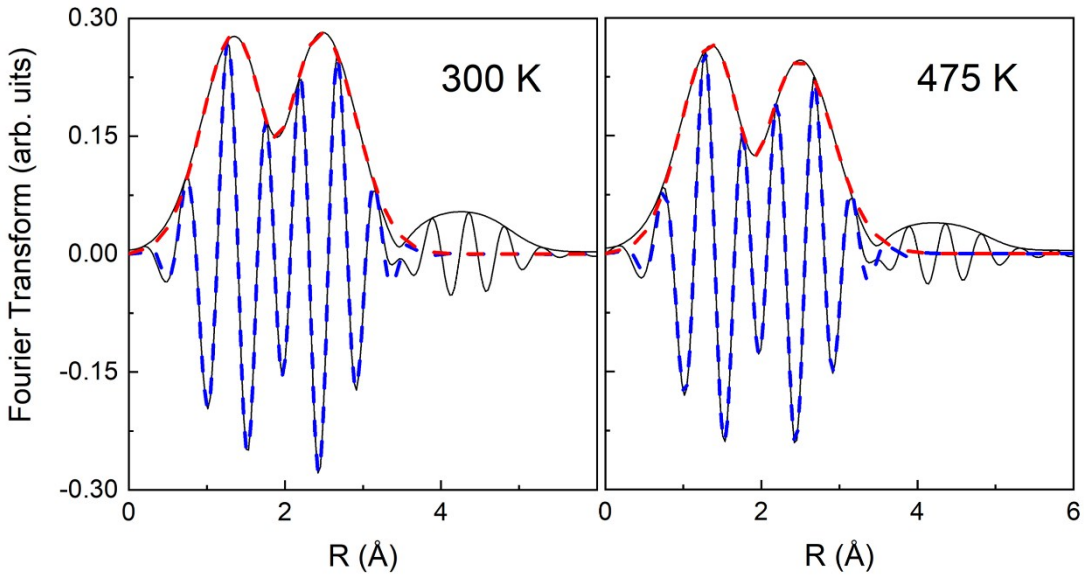

Figure S6. Modulus and imaginary part of the Fourier transform of Fe K-edge EXAFS signal of $FeFe(CN)_6$ (continuous lines) and best-fitting simulation of the first two peaks (dashed-bold lines) at room temperature (left panel) and 475 K (right panel).

Table S2. Scattering paths related to FT structure below ~3.5 Å of $FeFe(CN)_6$, calculated by FEFF code, [15] from Fe1 and Fe2 absorbing atoms. The last column lists the fitting parameters (distance, Debye-Waller factor and third cumulant) and the constraints used for each scattering path.

Index Fe1	**Path**	**Legs**	**Degeneracy**	**reff (Å)**	**Amplitude**	**Parameters**
1	Fe1-C	2	6	1.9441	100.00	$r_1, {\sigma_1}^2, C_{31}$
2	Fe1-N	2	6	3.1162	34.68	$r_2, 2{\sigma_1}^2$
3	Fe1-C-N	3	12	3.1162	158.10	$r_1/2 + r_2/2 + r_3/2$ ${\sigma_1}^2/2 + 2{\sigma_1}^2/2 + {\sigma_3}^2/2$
4	Fe1-C-N-C	4	6	3.1162	181.61	$r_1 + r_3$ ${\sigma_1}^2 + {\sigma_3}^2$
5	Fe1-C-C	3	24	3.3188	25.93	Neglected
Index Fe2	**Path**	**Legs**	**Degeneracy**	**reff (Å)**	**Amplitude**	**Parameters**
1’	Fe2-N	2	6	1.9765	100.00	$r_1', {\sigma_1}'^2, C_{31}$
2’	Fe2-C	2	6	3.1486	30.72	$r_2', 2{\sigma_1}'^2$
3’	Fe2-N-C	3	12	3.1486	141.62	$r_1'/2 + r_2'/2 + r_3/2$ ${\sigma_1}'^2/2 + 2{\sigma_1}'^2/2 + {\sigma_3}^2/2$
4’	Fe2-N-C-N	4	6	3.1486	171.49	$r_1' + r_3$ ${\sigma_1}'^2 + {\sigma_3}^2$
5’	Fe2-N-N	3	24	3.3741	26.04	Neglected

Table S3. Vibrational dynamics parameters of Fe-C and Fe-N atomic pairs measured by EXAFS in $FeFe(CN)_6$. $\nu_{||}$ and $\nu_{\perp}$ are the best-fitting Einstein frequencies of the parallel and perpendicular MSRDs, respectively; $k_{||}$ and $k_{\perp}$ are the corresponding bond-stretching and bond-bending effective force constants; γ represents the anisotropy of the relative thermal vibrations.

	Fe-C	**Fe-N**
$\nu_{||}$	14.55 ± 2.15 THz	22.77 ± 4.69 THz
$\nu_{\perp}$	4.61 ± 0.71 THz	3.60 +/- 0.44 THz
$k_{||}$	8.56 ± 2.53 eV/Å^2	23.76 ± 9.79 eV/Å^2
$k_{\perp}$	0.86 ± 0.26 eV/Å^2	0.594 ± 0.145 eV/Å^2

γ **at 475 K**	17.3 ± 5.1	57.5 ± 14.2

References

1 L. Hu, J. Chen, A. Sanson, H. Wu, C. Guglieri-Rodriguez, L. Olivi, Y. Ren, L. Fan, J. Deng and X. Xing, *J. Am. Chem. Soc.*, 2016, **138**, 8320-8323.

2 L. Hu, J. Chen, J. Xu, N. Wang, F. Han, Y. Ren, Zhao. P, Y. Rong, R. Huang, J. Deng, L. Li and X. Xing, *J. Am. Chem. Soc.*, 2016, **138**, 14530-14533.

3 C. Lind, A. P. Wilkinson, Z. Hu, S. Short and J. D. Jorgensen, *Chem Mater*, 1998, **10**, 2335-2337.

4 Q. Liu, X. Cheng, X. Sun, J. Yang and H. Li, *J Sol-Gel Sci Techn*, 2014, **72**, 502-510.

5 A. W. Sleight, *Annu. Rev. Mater. Sci.*, 1998, **28**, 29-43.

6 K. W. Chapman, P. J. Chupas and C. J. Kepert, *J. Am. Chem. Soc.*, 2006, **128**, 7009-7014.

7 D. J. Williams, D. E. Partin, F. J. Lincoln, J. Kouvetakis and M. O'Keeffe, *J. Solid. State. Chem.*, 1997, **134**, 164-169.

8 T. Matsuda, J. E. Kim, K. Ohoyama and Y. Moritomo, *Phys. Rev. B*, 2009, **79**, 172302.

9 Q. Gao, N. Shi, Q. Sun, A. Sanson, R. Milazzo, A. Carnera, H. Zhu, S. H. Lapidus, Y. Ren, Q. Huang, J. Chen and X. Xing, *Inorg. Chem.*, 2018, 57, 10918-10924.

10 A. L. Goodwin and C. J. Kepert, *Phys. Rev. B*, 2005, **71**, 140301.

11 (a) D. E. Sayers and B. A. Bunker. in X-ray Absorption: Principles, Applications, Techniques of EXAFS, SEXAFS and XANES, edited by D. C. Koningsberger and R. Prins. *Wiley, New York*, 1988. (b) Fornasini P in Synchrotron Radiation - Basics, Methods and Applications. edited by S. Mobilio, C. Meneghini and F. Boscherini. *Springer-Verlag, Berlin*, 2015. 181–211.

12 L. Ankudinov, B. Ravel, J. J. Rehr and S. D. Conradson, *Phys. Rev. B*, 1998, **58**: 7565.

13 M. Newville, B. Ravel, J. J. Rehr, E. Stern and Y. Yacoby, *Physica. B*, 1995, **208**: 154.

14 A. Sanson, *J. Synchr. Rad*, 2008, **15**: 514.

15 L. Ankudinov, B. Ravel, J. J. Rehr and S. D. Conradson, *Phys. Rev. B*, 1998, **58**: 7565.